BMC Oral Health

RESEARCH

Open Access

# The preventive effect of photocrosslinked Hep/GelMA hydrogel loaded with PRF on MRONJ

Lu Tao[1,2], Ying Gao[1,2], Yushen Li[1,2], Liuqing Yang[1,2], Jingjing Yao[1,2], Handan Huang[1,2], Jinling Yu[1,2], Bing Han[4*], Bowei Wang[3*] and Zhihui Liu[1,2*]

## Abstract

**Background** Medication-related osteonecrosis of the Jaw (MRONJ) is a rare but severe side effect in patients treated with medications such as Bisphosphonates (BPs). Its pathophysiological mechanism needs to be more precise. Establishing preventive measures and treatment standards is necessary. This study aimed to develop a composite hydrogel scaffold constituted by methacrylated gelatin (GelMA), methacrylated heparin (HepMA) and PRF, and investigate its potential application value in the prevention of MRONJ.

**Methods** GelMA, HepMA, and PRF were prepared using specific ratios for hydrogel scaffolds. Through mechanical properties and biocompatibility analysis, the release rate of growth factors and the ability to promote bone differentiation in vitro were evaluated. To explore the healing-enhancing effects of hydrogels in vivo, the composite hydrogel scaffold was implanted to the MRONJ rat model. Micro-computed tomography (Micro-CT) and histological examination were conducted to evaluate the bone morphology and tissue regeneration.

**Results** The Hep/GelMA-PRF hydrogel improved the degradation rate and swelling rate. It was also used to control the release rate of growth factors effectively. In vitro, the Hep/GelMA-PRF hydrogel was biocompatible and capable of reversing the inhibitory effect of zoledronic acid (ZOL) on the osteogenic differentiation of MC3T3-E1s. In vivo, the micro-CT analysis and histological evaluation demonstrated that the Hep/GelMA-PRF group exhibited the best tissue reconstruction. Moreover, compared to the ZOL group, the expression of osteogenesis proteins, including osteocalcin (OCN), type collagen I (Col I), and bone morphogenetic protein-2 (BMP-2) in the Hep/GelMA-PRF group were all significantly upregulated ($P < 0.05$).

**Conclusions** The Hep/GelMA-PRF hydrogel scaffold could effectively control the release rate of growth factors, induce osteogenic differentiation, reduce inflammation, and keep a stable microenvironment for tissue repair. It has potential application value in the prevention of MRONJ.

*Correspondence:
Bing Han
hanb@jlu.edu.cn
Bowei Wang
wangbw@jlu.edu.cn
Zhihui Liu
liu_zh@jlu.edu.cn

Full list of author information is available at the end of the article

**Keywords** Hydrogel, Medication-related osteonecrosis of the jaw, Bisphosphonates, Platelet-rich fibrin

## Introduction

Bisphosphonates (BPs), which chelate calcium ions on the surface of hydroxyapatite crystals through phosphonic acid groups, impair the absorption capacity and cell integrity of osteoclasts by blocking ATP synthesis of osteoclasts and inhibiting metabolic enzymes of the nervonic acid pathway, are the first-line drugs for the treatment of calcium metabolism disorders [1–3]. As a highly stable compound, BPs are not saturated at skeleton-binding sites in bone. Repeated administration of BPs in clinical practice will continuously accumulate bioactive doses in bone, forming a reservoir of adsorbed drugs, which will continue to be released for months or years after stopping treatment [4, 5]. It will affect the alveolar bone replacement cycle, destroy the osteogenesis-osteoclast balance, and make alveolar bone lose its ability to repair bone micro-damage, leading to regional osteonecrosis [6] (Fig. 1a). For better disease management, the American Association of Oral and Maxillofacial Surgeons (AAOMS) [7, 8] defined Medication-related osteonecrosis of the Jaw (MRONJ) as having been treated with BPs, and the maxillofacial region had persistent dead bone exposure of more than eight weeks and no history of radiotherapy.

Oral invasive procedures usually cause MRONJ. Tooth extraction is known to be the most important independent risk factor for MRONJ [7, 9]. However, the pathophysiological mechanism of MRONJ needs to be more precise. Moreover, unified prevention measures and treatment standards are needed. In particular, the prevention of the disease is crucial for cancer patients. Many researchers are trying to figure out how to solve this challenge. The development of some biomaterials is still in the preclinical modeling stage, and in vitro studies still need to be completed [10, 11].

In recent years, reports have emerged of platelet-rich fibrin (PRF) contributing to the treatment of MRONJ [12–14]. PRF is the second generation of APCs. It can release Platelet-derived growth factors (PDGF), Transforming growth factor β1 (TGF-β1), Vascular endothelial growth factor (VEGF), and so on. The growth factors can stimulate the production of collagen, produce anti-inflammatory agents, initiate internal growth of blood vessels, induce cell differentiation, control the local inflammatory response, and help tissue healing [15]. It has positive functions of soft tissue regeneration, plastic surgery, guided bone tissue regeneration, maxillary sinus lifting, skin graft healing, and other aspects [12]. Notably, Jamalpour et al. [16] treated the MRONJ rat model by surgery combined with PRF and photobiomodulation with efficacy in promoting wound healing and bone tissue regeneration. It is hypothesized that PRF may contribute to the prevention of MRONJ.

Collagen, mucopolysaccharide sulfate, and other natural materials exist widely and have good biocompatibility. Hydrogels are essential in cell culture, tissue engineering, and other fields. However, in addition to complementary functional group reactions, natural materials often rely on physical crosslinking and need better mechanical strength and stability. Methacrylic acid (MA) has recently been a widely used modification scheme. MA is used to modify the side chains of gelatin and heparin to obtain methacrylate gelatin (GelMA) and methacrylate heparin (HepMA) [17, 18]. It preserves the arginine-glycine-aspartic acid (RGD) and the matrix metalloproteinase (MMP) sequence on the main chain of gelatin. Moreover, HepMA preserves the ability of specific binding growth factors [19, 20]. At the same time, MA modification gives GelMA and HepMA the ability to covalently bond under ultraviolet light, which has higher stability than physical cross-linking (Fig. 1b).

Therefore, this experiment intended to combine PRF with the GelMA and HepMA mixed system to prepare a multi-component photocurable hydrogel, which could play a synergistic role. We established the MRONJ rat model through BPs administration and tooth extraction. The composite hydrogel was placed into the extraction socket to provide a physical barrier and help tissue regeneration (Fig. 1c). We evaluated the preventive effect of Hep/GelMA-PRF hydrogel on MRONJ by observing the wound healing after tooth extraction in rats.

## Result

### Morphological assessment

After irradiating under UV light at 405 nm, GelMA appeared as light yellow (Fig. 2a, e). Hep/GelMA appeared as colorless (Fig. 2b, e). GelMA-PRF was orange (Fig. 2c, e). Hep/GelMA-PRF was reddish-orange (Fig. 2d, e).

### FT-IR assessment

The absorption peak at 3421 $cm^{-1}$, the amide A band, is due to the stretching vibration of the N-H and O-H groups. The absorption peak at 2978 $cm^{-1}$, the amide B band, is due to the C-H group stretching. The absorption peak at 1615 $cm^{-1}$ is associated with C=O stretching, which is the amide I band. The absorption peak at 1545 $cm^{-1}$ is attributed to N-H bending, the amide II band. The absorption peak at 1390 $cm^{-1}$ is related to the N-H bending vibration, the amide III band. Hep/GelMA hydrogels have similar peak patterns to GelMA and HepMA (Fig. 3a).

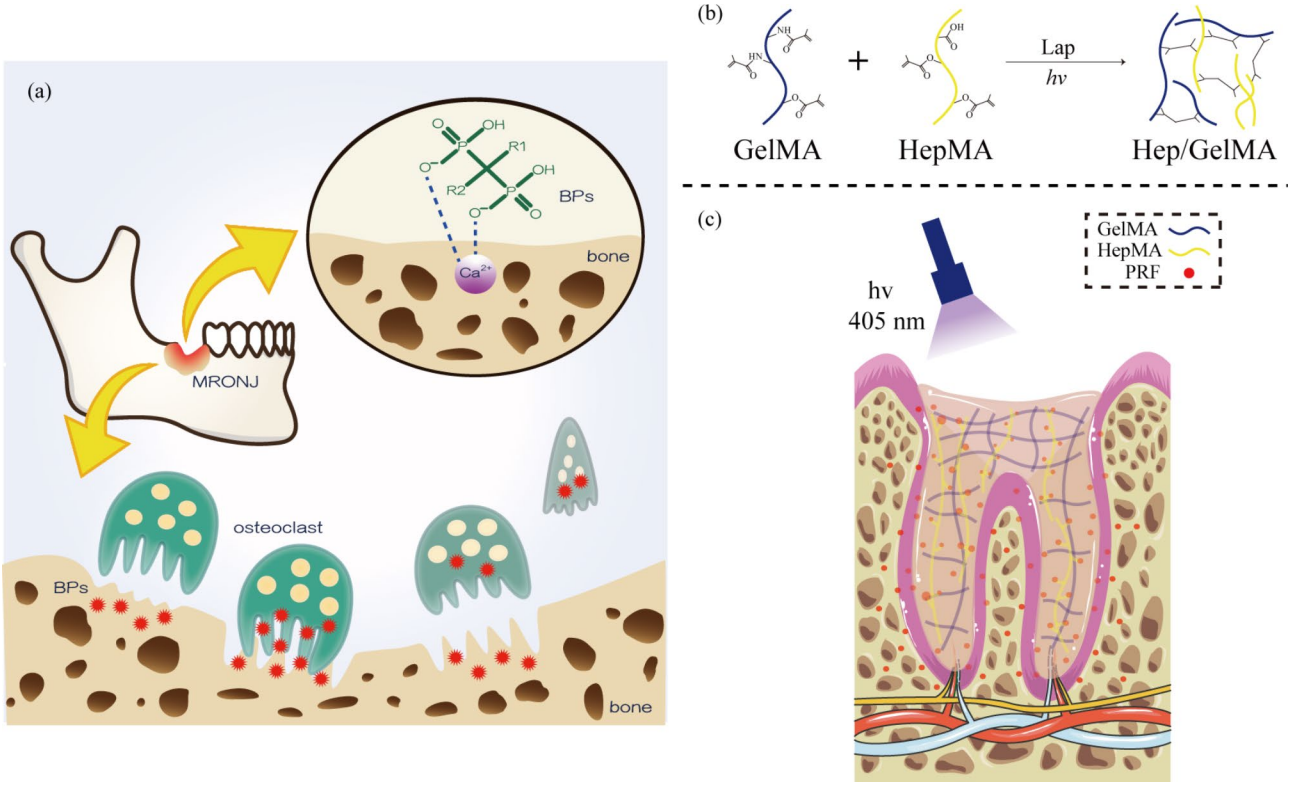


**Fig. 1** Mechanism diagram. (**a**) BPs cause MRONJ. The P-C-P structure of the main chain of BPs forms a bidentate chelator by chelating calcium ions on the surface of bone apatite crystals through two adjacent phosphonic acid groups, which can create a strong bond with the HA crystal. BPs are released into the cytoplasm of osteoclasts after separation from HA in the vesicles of osteoclasts and inhibit bone resorption by blocking ATP synthesis, inhibiting metabolic enzymes of the mevalonate pathway, impairing the resorptive capacity and cell integrity of osteoclasts, and triggering apoptosis. (**b**) GelMA Crosslinks with HepMA through ultraviolet light. (**c**) Hep/GelMA-PRF solution is solidified into a hydrogel in the extraction socket by ultraviolet light. PRF can release growth factors in the extraction socket.

#### Critical electrolyte concentration staining assessment

Compared to Hep/GelMA, GelMA showed a lighter blue color in Alcian Blue stains at >0.05 M $MgCl_2$ concentration. However, Hep/GelMA showed a dark blue color from 0.05 M to 0.5 M. There was no significant difference in the staining intensity of the two hydrogels in the 0.7–0.9 M $MgCl_2$ concentration of the staining solution (Fig. 3b).

#### Degradation rate and growth factor sustained-release capacity assessment

The degradation of hydrogels increased with time in all groups (Fig. 3c). GelMA showed rapid degradation, with scaffold structure breakage occurring after 7–14 days. Its complete degradation takes about 21 days. The rapid degradation of GelMA-PRF appeared within 5–7 days, earlier than that of GelMA. Whatmore its complete degradation takes about 14 days. Hep/GelMA and Hep/GelMA-PRF degraded slowly and steadily over 28 days, with only partial degradation. In addition, Hep/GelMA-PRF hydrogel can release PRF growth factors continuously for more than four weeks (Fig. 3d).

#### Swelling balance assessment

The results showed a gently rising trend of GelMA-PRF and Hep/GelMA-PRF. They reached the swelling balance after 24 h. However, GelMA maintained a steady upturn. At 48 h, the swelling rate of GelMA-PRF and Hep/GelMA-PRF was less than that of GelMA and Hep/GelMA (Fig. 3e).

#### Biocompatibility assessment

MC3T3-E1 were distributed in the bottom of the petri dish. They were fusiform, showing a positive growth state (Fig. 4a).

The live/dead staining tested the biocompatibility of the hydrogel (Fig. 4b). The cells showed high proliferative activity and a low proportion of dead cells (red) in each group. All the hydrogels showed no cytotoxicity and good biocompatibility. The number of cells in each group increased gradually over time. On day 3, the proportion of living cells in the Hep/GelMA-PRF group and GelMA-PRF group was significantly higher than that in the other two groups, indicating that the hydrogels in the two groups were more vital in promoting the proliferation of MC3T3-E1.

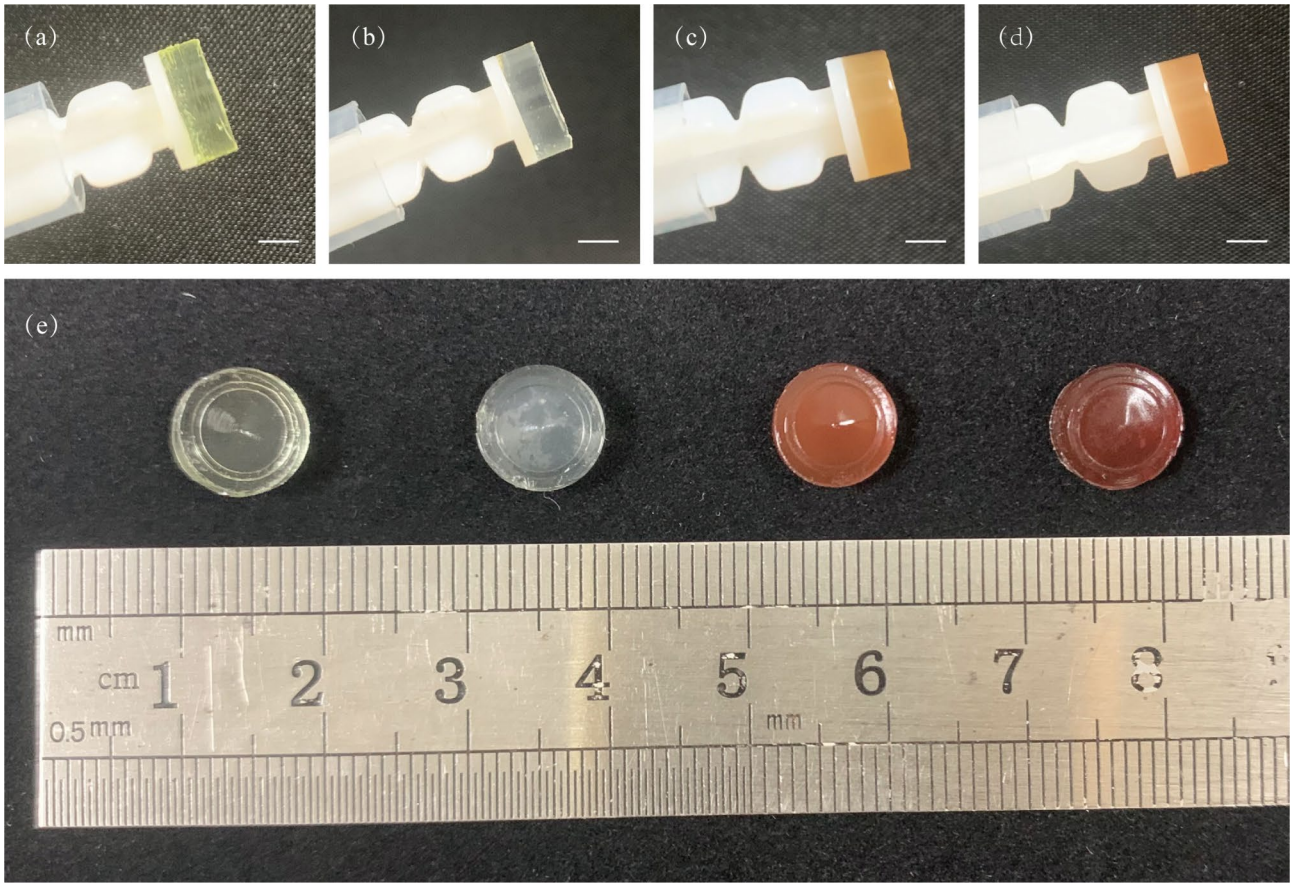


**Fig. 2** Morphological assessment. (**a**) GelMA. (**b**) Hep/GelMA. (**c**) GelMA-PRF. (**d**) Hep/GelMA-PRF. (**e**) From left to right: GelMA、Hep/GelMA、GelMA-PRF、Hep/GelMA-PRF. (Scale bar: 3 mm)

CCK-8 staining detected the effect of zoledronic acid (ZOL) on the proliferation of MC3T3-E1 (Fig. 4c). As shown in picture 4c, compared with the 0 μmol/L ZOL group, the 2 μmol/L group could significantly inhibit cell proliferation on day 5. Therefore, 2 μmol/L ZOL was selected for the subsequent experiment.

ZOL-induced MC3T3-E1 cocultured with hydrogels. CCK-8 staining detected the cells' proliferative activity (Fig. 4d). The results showed that the proliferating activity of the Hep/GelMA-PRF+ZOL group was significantly higher than that of the GelMA+ZOL group ($P<0.05$). It was confirmed that Hep/GelMA-PRF hydrogel could resist the inhibitory effect of ZOL on the proliferation of MC3T3- E1.

ZOL-induced MC3T3-E1 cocultured with hydrogel extract. Moreover, the activity of cells in each group was observed by the live/dead staining (Fig. 4e). The live/dead staining showed that the proportion of dead cells in the ZOL group was significantly higher than in the other three groups on day 3. Furthermore, compared with the ZOL group, the Hep/GelMA-PRF+ZOL group had significantly stronger green fluorescence per unit area. In conclusion, the Hep/GelMA-PRF+ZOL group had a higher proportion of living cells, better cell vitality, and could resist the negative effect of ZOL.

#### Osteogenic differentiation assessment

On day 7, ALP staining showed that the Hep/GelMA-PRF group was more profound than the GelMA group (Fig. 4f). Moreover, The Hep/GelMA-PRF+ZOL group was more profound than the GelMA+ZOL group. On day 14, the Hep/GelMA-PRF+ZOL group was still more profound than the GelMA+ZOL group. These results indicated that Hep/GelMA-PRF could induce early osteogenic differentiation and resist the inhibitory effect of ZOL.

Alizarin red staining was performed on MC3T3-E1 (Fig. 4g). The Hep/GelMA-PRF group formed more calcium nodules than the other three groups. However, no apparent calcium nodules were found in the GelMA and the GelMA+ZOL groups. The cells in the GelMA+ZOL group shrank and became round, which may be caused by the toxic effect of ZOL. There were more calcium nodules in the Hep/GelMA-PRF+ZOL group than in the GelMA+ZOL group. In conclusion, The Hep/

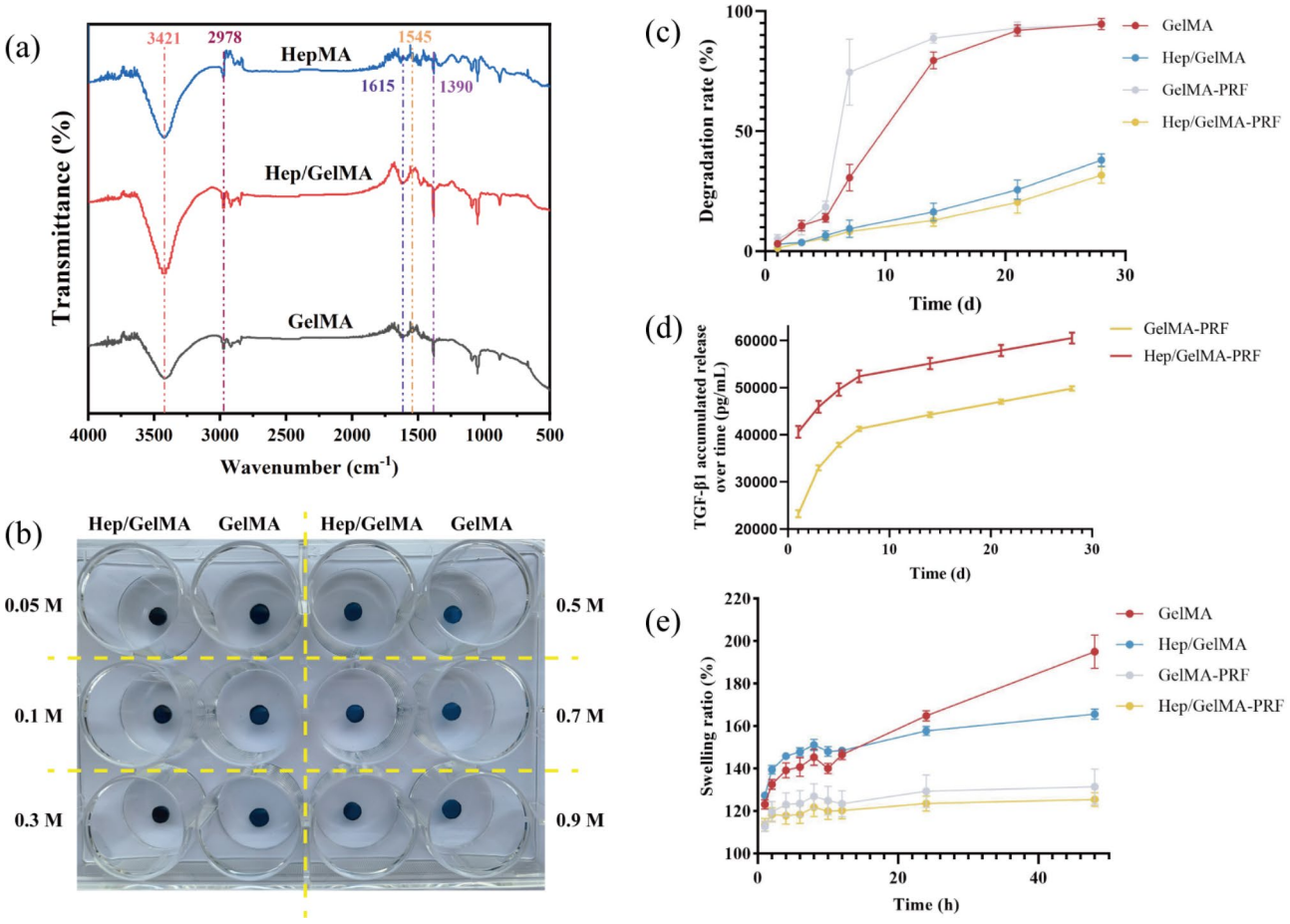


**Fig. 3** Characterization of hydrogels. (**a**) Fourier transform infrared spectrum. (**b**) Critical electrolyte concentration staining. Compared to Hep/GelMA, GelMA showed a lighter blue color in Alcian Blue stains at > 0.05 M $MgCl_2$ concentration. (**c**) Degradation rate. (**d**) Capacity of release of TGF-β1. (**e**) Swelling balance. Data represent mean ± SEM

GelMA-PRF hydrogel could reverse ZOL's inhibitory effect on osteogenic differentiation.

### Clinical assessment

The gingival in the control and Hep/GelMA-PRF groups was healing. However, the wound healing was delayed with yellow pus in the ZOL group at four weeks. Moreover, it had a large area of necrotic bone with gingival inflammation at eight weeks. And the Hep/GelMA group showed a small area of necrotic bone (Fig. 5a). Statistical analysis showed that the Hep/GelMA-PRF group significantly reduced the area of open wounds at four and eight weeks after tooth extraction compared with the ZOL group ($p<0.05$) (Fig. 5b).

### Radiographic assessment

X-ray and micro-CT were used to observe the bone tissue (Fig. 5c). The control group had horizontal resorption of the alveolar bone. At four weeks, the other three groups effectively preserved the alveolar bone, and there were apparent bone trabeculae in the proximal extraction sockets. The Hep/GelMA-PRF group had the most significant newborn bone trabeculae. Distal extraction sockets have a slower growth rate due to their big and deep size. However, by eight weeks, the ZOL group showed diffuse osteolytic destruction, blurred borders, and dead bone fragments. It also expanded the bone toward the buccal and lingual sides. The Hep/GelMA and the Hep/GelMA-PRF groups effectively healed the wounds. The Hep/GelMA-PRF group had the most significant healing effect, with the newborn bone trabeculae maturing and being able to fill the extraction sockets.

Statistical analysis showed that the BV/TV and the BMD of the Hep/GelMA-PRF group were significantly higher than the ZOL group at eight weeks ($P<0.05$) (Fig. 5d, e). The Tb.Sp of the Hep/GelMA-PRF group was significantly lower than the ZOL group at eight weeks ($p<0.05$) (Fig. 5f). Meanwhile, the Tb.Th of the Hep/GelMA-PRF group in eight weeks was significantly increased compared to four weeks ($P<0.05$) (Fig. 5g).

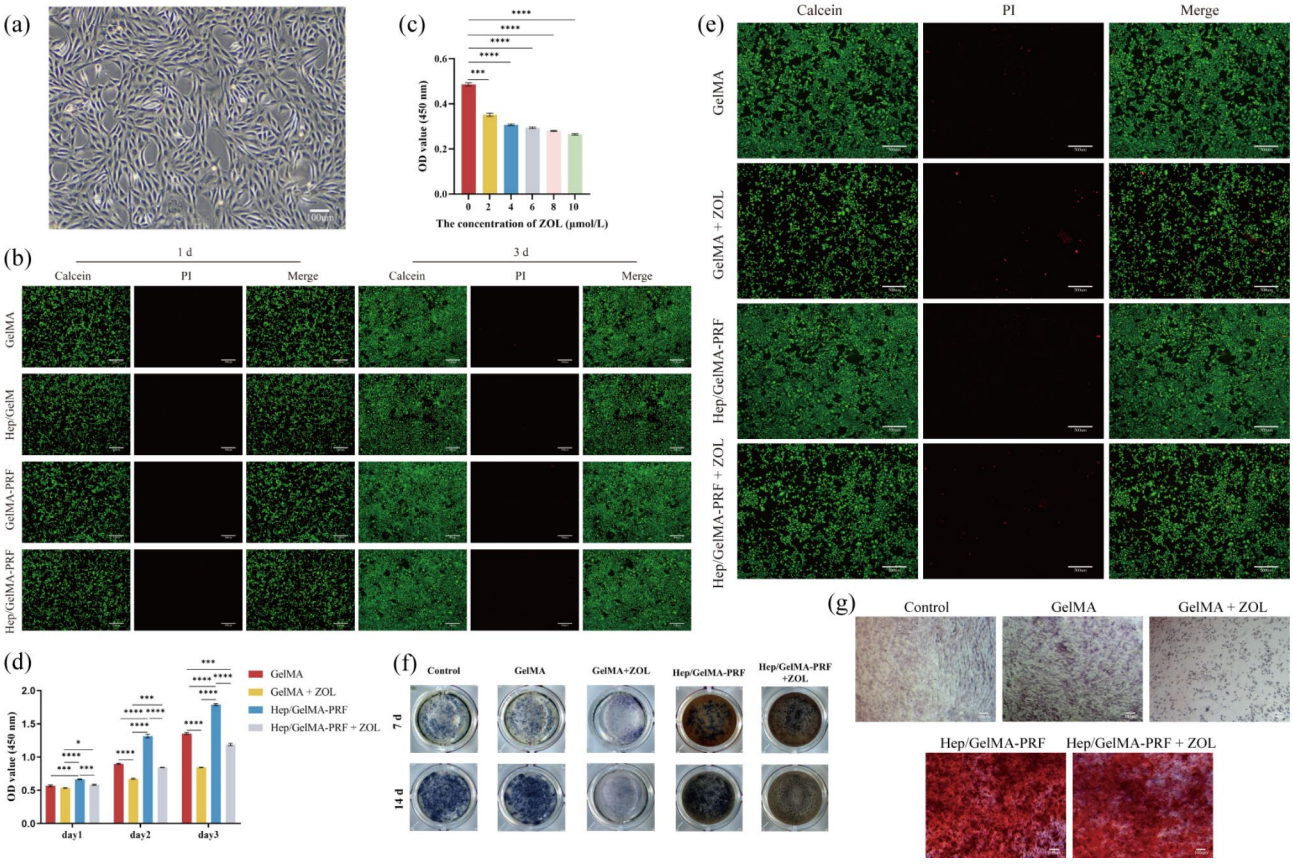


**Fig. 4** In vitro assessment. (**a**) MC3T3-E1. (Scale bar: 100 μm) (**b**) Live/dead staining was used to test the biocompatibility of hydrogels. (Scale bar: 500 μm) (**c**) CCK-8 staining was used to screen for ZOL concentration. (**d**) CCK-8 staining was used to detect ZOL-induced cell proliferative activity. (**e**) Live/dead staining assay was performed to detect ZOL-induced cell proliferative activity. (Scale bar: 500 μm) (**f**) ALP staining. (**g**) Alizarin red staining. (Scale bar: 100 μm) Data represent mean ± SEM. (*: $p < 0.05$, **: $p < 0.01$, ***: $p < 0.001$, ****: $p < 0.0001$)

### Histologic assessment

At four weeks, many empty lacunae and neutrophils appeared in the ZOL group, suggesting extensive necrotic bone tissue and diffuse inflammatory infiltration. The crest of the alveolar ridge, especially the interradicular septa, concentrated most empty lacunae. The control and Hep/GelMA-PRF groups had no inflammation and empty lacunae. However, the control group had severe bone absorption. In contrast, the Hep/GelMA-PRF group formed many new braided bones and small blood vessels.

At eight weeks, the ZOL group inhibited bone remodeling and formed some sequestrum with inflammation and colony infections. The Hep/GelMA group also formed empty lacunae and inflammation. In contrast, the Hep/GelMA-PRF group formed new bones with no prominent inflammation and empty lacunae (Fig. 5h).

Statistical analysis showed that the bone-filling percentage of the Hep/GelMA-PRF group was significantly higher than that of the other three groups ($P<0.05$) (Fig. 5i). In addition, the necrotic bone area of the ZOL group was significantly higher than that of the other three groups ($P<0.05$) (Fig. 5j).

Masson staining showed dense, thick, and regular collagen fibers in the control and Hep/GelMA-PRF groups. The ZOL group had fewer collagen fibers with severe inflammation and colony infections (Fig. 6a).

Osteoclasts can be stained purple-red by the TRAP (Fig. 6b). At four weeks, the number of osteoclasts was higher in the Hep/GelMA-PRF group ($P<0.05$). At eight weeks, there was a significant increase in the ZOL group ($P<0.05$) (Fig. 6c).

Immunohistochemical staining showed that at four weeks, the Hep/GelMA-PRF group expressed more OCN-positive protein, Col I-positive protein, and BMP-2-positive protein than the ZOL group ($P<0.05$) (Fig. 6d, e, f, g). The control group had the highest expression of VEGF-positive protein. At eight weeks, the control, Hep/GelMA, and Hep/GelMA-PRF groups expressed less Col I-positive protein ($P<0.05$) (Fig. 6d, f). In addition, the control and Hep/GelMA-PRF groups expressed less VEGF-positive protein ($P<0.05$) (Fig. 6d, h).

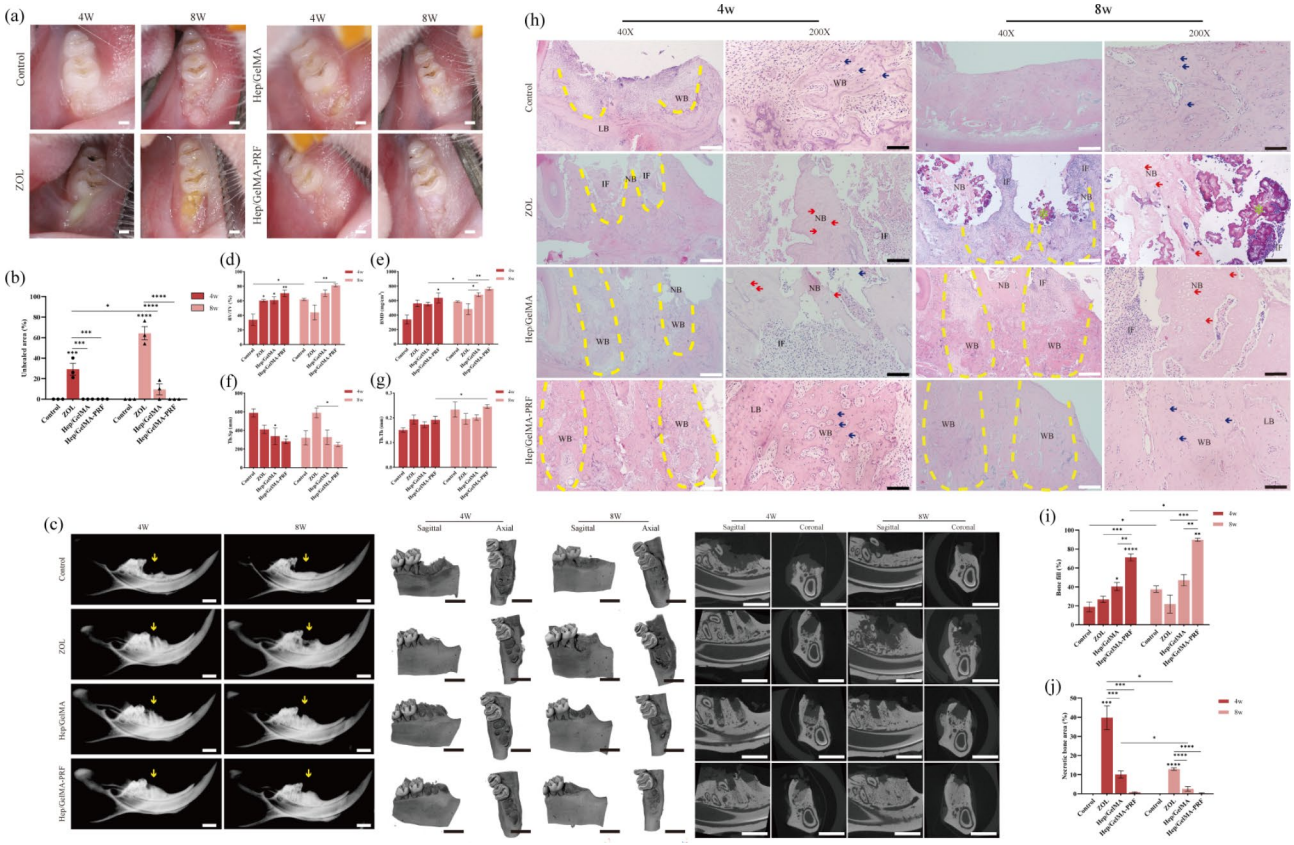


**Fig. 5** In vivo assessment. (**a**) Post-treatment clinical results. (Scale bar: 1 mm) (**b**) The percentage of unhealed areas. (**c**) Radiographic assessment. (Yellow arrow: extraction fossa) (Scale bars: 3 mm) (**d-g**) Bone metabolism-related indexes of each group. (**d**) BV/TV. (**e**) BMD. (**f**) Tb.Sp (**g**) Tb.Th. (**h**) Histologic assessment. WB: Woven bone. LB: Lamellar bone. NB: Necrotic bone. IF: Inflammatory infiltration. red arrow: empty lacunae. blue arrow: osteocytes. *: bacterial colony. (White scale bar: 500 μm. black scale bar: 100 μm) (**i**) Bone filling percentage. (**j**) Necrotic bone area percentage. Data represent mean ± SEM. (*: $p < 0.05$, **: $p < 0.01$, ***: $p < 0.001$, ****: $p < 0.0001$)

## Discussion

BPs are first-line agents for treating disorders of calcium metabolism. They are widely used to treat patients suffering from bone tumors, osteoporosis, Paget's Disease (PD), acute hypercalcemia, and multiple myeloma [21]. However, prescriptions for BPs in the U.S. fell by nearly seven million after introducing MRONJ [22]. The prevention and treatment of MRONJ is a complex problem that needs to be solved, and millions of patients worldwide still need to take BPs for various diseases.

PRF is a second-generation APC rich in several growth factors. It can stimulate collagen production, initiate intravascular growth, and control local inflammatory responses. However, PRF degrades rapidly. The release time of growth factors can only last seven days, and its long-term efficacy in preventing and treating MRONJ remains to be further investigated [23]. Based on this, the construction of PRF-loaded hydrogel scaffold materials is expected to delay the release time of growth factors.

As described by Scott et al. [24], the critical electrolyte staining method selectively stains anionic functional groups based on the $MgCl_2$ concentration. Thus, sulfate groups can be colored at higher magnesium ion concentrations than carboxylate groups. Due to the presence of carboxyl and sulfate groups in HepMA and only carboxyl groups in GelMA, Hep/GelMA hydrogels can take on a darker blue color in higher concentrations of electrolyte solutions, but GelMA hydrogels have a lighter blue color.

The hydrophilicity and water absorption of hydrogels are related to the crosslinked network's molecular structure and the monomers' degree of crosslinking. If the crosslinked network is too tightly structured, the hydrogel's water absorption is reduced. The higher the hydrophilicity of the monomer structure, the better the water absorption of the hydrogel. In the swelling balance test, the PRF-loaded hydrogels reached the swelling balance within 12–24 h, suggesting that incorporating PRF and HepMA made the crosslinked network structure more compact and stable.

Crosslinking is the key to avoiding the dissolution of hydrophilic polymer chains. The Hep/GelMA-PRF hydrogel maintained a low degradation rate within 28 d, indicating that the incorporation of HepMA increased the stability of the crosslinking system and prolonged the

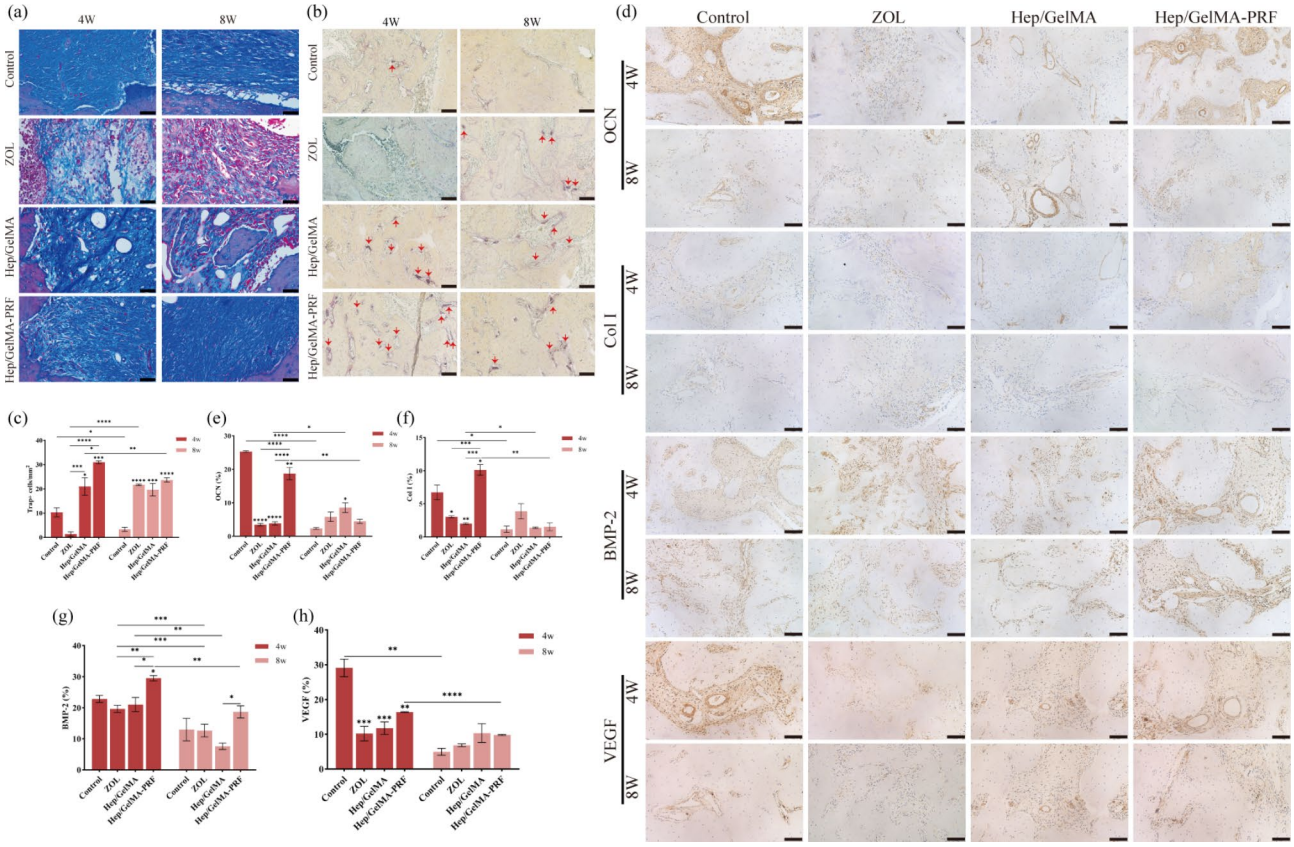


**Fig. 6** In vivo assessment. (**a**) Masson staining. (Scale bar: 50 μm) (**b**) Trap staining. (Red arrow: osteoclast) (Scale bar: 100 μm) (**c**) Trap + cell number / $mm^2$ in each group. (**d**) Immunohistochemical staining. (Scale bar: 100 μm) (**e-h**) Immunohistochemical protein expression. (**e**) OCN. (**f**) Col I. (**g**) BMP-2. (**h**) VEGF. Data represent mean ± SEM. (*: $p < 0.05$, **: $p < 0.01$, ***: $p < 0.001$, ****: $p < 0.0001$)

degradation time of the hydrogel. This confirms that the dense and firm three-dimensional network of the Hep/GelMA-PRF hydrogel could firmly bind the PRF in the hydrogel, realizing the long-term and sustained release of the growth factors.

Researchers have developed various preclinical models to explore the mechanisms of MRONJ. Rats are the most frequently used animal in the MRONJ model (up to 60%) due to general advantages such as ease of husbandry, shorter experimental period, and lower costs [25]. Systemic drug induction combined with tooth extraction is the most common combination in the model. ZOL is a third-generation BPs, the most potent and longest-lasting BPs in the clinic, and is the most common choice in the MRONJ model [26]. The AAOMS definition stipulates that a diagnosis of MRONJ requires "persistent exposure to the sequestrum for more than eight weeks or a fistula deep to the sequestrum, " equivalent to one week of rat life [7, 8]. Therefore, MRONJ-like lesions should be present in rats for at least one week to verify the successful establishment of the model. An ideal model should mimic the pathophysiological features of MRONJ, including osteonecrosis, inflammation, and angiogenesis inhibition. However, the current model only simulates some of these pathophysiological features [25]. Our study concluded that MRONJ-like lesions could exist in rats for over one week, and the MRONJ model was considered successful.

The ZOL group had delayed healing with necrotic bone exposure and gingival inflammation, so the MRONJ model was established successfully. Meanwhile, the Hep/GelMA-PRF group showed tissue regeneration.

On radiographic assessment, the ZOL group showed increased sequestrum and higher Tb.Sp values than the Hep/GelMA-PRF group. It suggests that bone trabeculae were less connected, and bone integrity was disrupted in the ZOL group. Which is an essential indicator for evaluating MRONJ [27]. The Hep/GelMA-PRF group increased BV/TV and BMD values compared with the ZOL group. Notably, the alveolar bone in the control group was gradually resorbed. In contrast, the other groups could maintain the morphology of the extraction sockets, which was speculated to be related to the ZOL-inhibiting bone resorption mechanism. In addition, the hydrogel covering the wound provided a stable microenvironment for blood clot mechanization and tissue regeneration.

Histologic assessment can observe more severe lesions. Sequestrum formation is the most important marker of the MRONJ rat model. In general, necrotic bone is an area with at least ten contiguous empty lacunae [27, 28]. In this experiment, HE staining showed large areas of empty lacunae in the ZOL and Hep/GelMA groups. These were mainly concentrated at the top of the alveolar ridge, especially at the root bifurcation, consistent with Yu et al.'s [29] findings. We suppose that the surgery damaged the alveolar ridge, forming a sequestrum. ZOL impaired the resorption function of osteoclasts, and the organism failed to remove the sequestrum in time. Second, ZOL decreased the number of endothelial cells and endothelial precursor cells, which could easily trigger ischemic necrosis. The location of the alveolar ridge was far away from the mandibular neural tube, so there was not enough blood supply. Meanwhile, the necrotic bone was exposed and infected, so this area was the first to develop osteonecrosis.

In addition, ZOL inhibited bone formation by impairing osteoclast resorption and osteoclast-osteoblast balance [30, 31]. In the absence of any new bone formation on the surface of the existing bone, which became the primary source of new bone production in the extraction sockets, a clear boundary between the alveolar bone and the new woven bone was observed in the histologic assessment (Fig. 5). It is suggested that Hep/GelMA-PRF hydrogel mediates woven bone formation by promoting such a bone formation pathway.

The oral mucosa surrounds the alveolar bone. The simultaneous healing of both after trauma is osteomucosal healing [32]. However, bone resorption and collagen formation play essential roles in the formation of new bone and connective tissue, which are critical steps in osteomucosal healing [32]. In this study, incomplete resorption of necrotic bone in the ZOL and Hep/GelMA groups affected osteomucosal healing and led to MRONJ. In contrast, collagen fibers of the Hep/GelMA-PRF group were deposited on the woven bone. At the same time, the epithelial cells migrate to the connective tissue and close the gingival, resulting in complete osteomucosal healing.

In addition, osteogenesis-related factors (OCN, Col I, BMP-2) and vasculogenesis-related factors (VEGF) are essential indicators of osteogenic and vasculogenic capacity, respectively. The upregulation of the expression of osteogenesis-related factor-positive proteins suggests that the Hep/GelMA-PRF group can promote the neogenesis of woven bone by promoting the expression of bone formation-related genes. However, there was no significant difference in VEGF-positive protein expression among the three groups injected with ZOL. PRF is rich in VEGF, which promotes angiogenesis [15]. However, hypoxia is a significant factor in VEGF production [33]. So, the expression of VEGF-positive protein increased in the ZOL and Hep/GelMA groups in infected and hypoxic environments.

In conclusion, this study successfully constructed the MRONJ rat model, and surgery, infection, and insufficient blood supply may be the triggering factors of MRONJ. The Hep/GelMA-PRF hydrogel has good biocompatibility and tissue regeneration ability. It rapidly activated the repair program, providing a stable microenvironment for repairing wounds, promoting osteomucosal healing, and avoiding sequestrum formation. The gingival of the Hep/GelMA-PRF group was regeneration. The hydrogel and the gingival prevented bacteria from invading and reduced infection. Moreover, releasing growth factors in the hydrogel promoted intravascular growth and controlled local inflammatory responses. At the same time, the hydrogel also acted as a barrier membrane, preventing gingival epithelial fibroblasts from growing into the extraction sockets. It could increase osteoblasts in the extraction sockets, providing a scaffold for bone regeneration.

In many case reports and a few clinical trials on MRONJ, the PRFs' application combined with other treatments has shown promising results [34, 35]. According to the previous preclinical study, PRF combined with photobiomodulation (PBM) treatment significantly improved clinical, histological, and radiographical parameters in MRONJ rat lesions [16]. However, they did not research the preventive effect of PRF on MRONJ. This study innovatively prepared the PRF composite hydrogel. It proved that Hep/GelMA-PRF hydrogel could effectively prevent the occurrence and progression of MRONJ in SD rats without other treatment. It provides a new idea for the prevention of MRONJ.

Although the results of this study presented significant differences in the prevention of the MRONJ rat model by Hep/GelMA-PRF composite hydrogels, there are still some limitations. The AAOMS suggests the prophylactic use of antibiotics after tooth extraction [8]. Antibiotics and antibacterial mouthwashes have many applications but are combined with other treatments [36]. According to recent research, PRF loaded with antibiotics allowed the release of antimicrobial drugs in an effective concentration [37]. Directly targeting tissues with local drug delivery strategies is a viable approach to reducing unnecessary antimicrobials. This may be one of the directions for future improvement of Hep/GelMA-PRF hydrogels. Further investigation is needed to illustrate the specific molecular mechanism of the prevention effects on MRONJ. In the future, the potential of Hep/GelMA-PRF hydrogels in the prevention of MRONJ needs to be further explored by large animal experiments to determine the efficacy and safety of this hydrogel.

## Materials and methods

### Animal care

Carried out all animal-related experiments in the Laboratory Animal Center of Jilin University. Reviewed and approved all experiments by the Institutional Animal Care and Use Committee and complied with Jilin University's and the state's requirements for the ethical welfare of experimental animals (China, Protocol number: SYXK2023-0010). Controlled the breeding conditions in strict accordance with GB14925.

### Preparation of L-PRF

Selected healthy adult female Sprague-Dawley (SD) rats weighing 200–220 g as the blood supply (Fig. 7a). After euthanized with an overdose of phenobarbital sodium salt, 5 ml of abdominal aortic blood was placed in additive-free glass tubes and then centrifuged at 400 g for 12 min. After standing at 4℃ for 2 min, take the middle layer of light yellow gel (Fig. 7b, c). After lyophilization, ground into powder and stored at -20℃ (Fig. 7d).

### Preparation of Hep/GelMA-PRF

HepMA (EFL, China) was added to the 0.25% (w/v) LAP solution (EFL, China) and heated in a water bath at 90℃ away from light. GelMA (GM-60, EFL, China) was added to the above solution and heated in a water bath at 40℃ to prepare the 1% (w/v) HepMA-10% (w/v) GelMA hydrogel precursor solution. A 0.22 μm sterile needle filter sterilized the solution. The lyophilized PRF powder was added to the precursor solution. The solution was irradiated under 405 nm ultraviolet light for 1 min and solidified into Hep/GelMA-PRF hydrogel (Fig. 7a).

### Fourier transform infrared spectrometer

2 mg of sample and 200 mg of KBr (Aladdin, China) were ground in an agate mortar of about 200 mesh. The polished sample was put into the infrared particular mold and pressed 12 Mpa on the tablet. Then, the sample was put in the instrument sample room. The detection range of the Fourier transform infrared spectrometer was 500–4000 $cm^{-1}$.

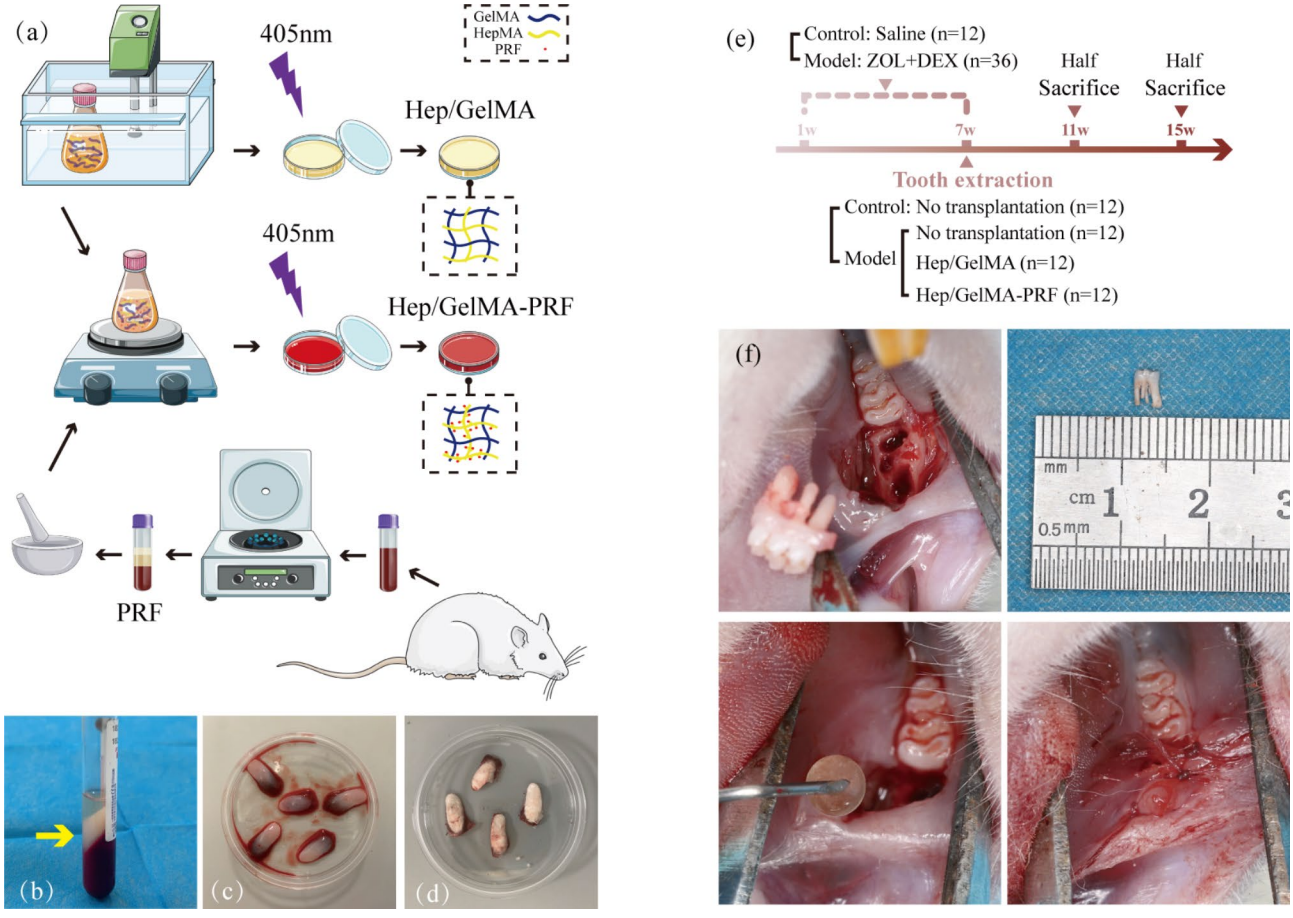


**Fig. 7** Experimental flow chart. (**a**) The preparation of Hep/GelMA-PRF. (**b**, **c**) Freshly extracted PRF (yellow arrow). (**d**) Lyophilized PRF. (**e**) Study groups. (**f**) Surgical flowchart. A sharp probe was wedged into the root bifurcation of the first mandibular molars to extract it, and the hydrogel was put in the tooth extraction fossa. Sutured the tooth socket

#### Critical electrolyte concentration staining

As described by Scott et al. [24], the samples were put into 1 mL of Alsin Blue dye (Solaibio, china) containing $MgCl^{2+}$ (0.05 M, 0.1 M, 0.3 M, 0.5 M, 0.7 M, 0.9 M) with different concentrations, and shaken overnight at room temperature, away from light. HepMA binding in hydrogels was verified by comparing staining intensity at different electrolyte concentrations.

#### Degradation rate determination

The lyophilized samples were weighed as W3. Then, the samples were soaked in 5 mL PBS at 1, 3, 5, 7, 14, 21, and 28 days, respectively, and weighed the degraded samples as Wd after lyophilization. The degradation rate was calculated as follows:

$$\text{Degradation rate}\,(\%) = \frac{\text{W3} - \text{Wd}}{\text{W3}} \times 100$$

W3 represents the weight of the lyophilized hydrogel. Wd represents the weight of lyophilized hydrogel after degradation.

#### Determination of growth factor sustained-release capacity

The sample was put in the 10 mL centrifuge tube, and 4 mL PBS was put into the incubator at 37℃. 2 mL supernatant PBS was collected at 1, 3, 5, 7, 14, 21, and 28 days, respectively. After that, the same volume of PBS was added. The TGF-β1 concentration in the supernatant at different times was determined by an ELISA kit (ABclonal, china) to evaluate hydrogel's growth factor sustained-release ability.

#### Swelling balance measurement

The fresh samples were weighed as W0. They were also immersed in 5 mL PBS and taken out at 0.5, 1, 2, 4, 6, 8, 12, 24, and 48 h and weighed as Wt. The swelling rate is the percentage between the swelling gel's weight and the fresh gel's weight. The formula is as follows.

$$\text{Swelling balance}\,(\%) = \frac{\text{Wt}}{\text{W0}} \times 100$$

Wt represents the weight of hydrogel after t hours of swelling. W0 represents the weight of the freshly prepared hydrogel.

#### Biocompatibility assessment

The extracts of the hydrogels were prepared according to the method of detecting biological materials provided by ISO10993-5. MC3T3-E1 were inoculated into the 24-well plates. After 24 h, the medium was discarded and replaced with the extracts. After 1 and 3 days, the cells were stained with a Calcein-AM/PI detection kit (Beyotime, China).

To investigate the effect of different concentrations of ZOL (Sinopharm, China) on cell proliferation, MC3T3-E1 were inoculated in the medium. After 24 h, the medium was replaced with the medium containing 0, 2, 4, 6, 8, and 10 μmol/L ZOL. CCK-8 (Ncmbio, China) was incubated for one hour. Then, the enzyme-labeled instrument measured the absorbance (Rayto, USA). The appropriate concentration of ZOL was selected for subsequent experiments.

MC3T3-E1 were inoculated on the hydrogel surface and put into the ZOL medium after 24 h. After 1, 2, and 3 days, the cells with CCK-8 were incubated for 2 h, and each well's absorbance value was measured.

MC3T3-E1 were inoculated in the medium, which were replaced with ZOL the next day. After three days, the cells were stained with a Calcein-AM/PI detection kit and observed under a fluorescence microscope.

#### Osteogenic differentiation assessment

MC3T3-E1 were inoculated on the hydrogel surface, and on the next day, the medium was changed to an osteogenic induction medium with or without ZOL. The elemental composition of the osteogenic induction medium was 50 μg/mL vitamin C+10 nM dexamethasone+5 mM β-sodium glycerophosphate-complete medium. The osteogenic induction medium was replaced with or without ZOL every three days. On the 7th and 14th day of osteogenic induction, the cells were stained with BCIP/NBT Alkaline Phosphatase Color Development Kit (Beyotime, china).

MC3T3-E1 were co-cultured with hydrogel after 28 days, and the cells were fixed with 4% paraformaldehyde at room temperature for 15 min on the gel surface. The cells were added to Alizarin Red S Solution (Solaibio, china) at room temperature for 30 min, then were observed under a microscope (OLYMPUS, Japan).

#### MRONJ rat model

Forty-eight female SD rats were selected, aged eight weeks, weighing 200–220 g. All mice were fed with sterile water, day and night alternations every 12 h, and adaptive feeding for one week. Thirty-six rats were selected. Throughout the experiment, they received intraperitoneal (IP) injections of 125 μg/kg ZOL two times weekly and 5 mg/kg dexamethasone (Dex; Chenxin Pharmaceutical Co., LTD, China) one time weekly. After six weeks, rats were euthanized with an overdose of phenobarbital sodium salt (Dingguo, china). Then, a sharp probe was wedged into the root bifurcation of the first mandibular molars to extract it, and the hydrogel was put in the tooth extraction fossa. Randomly divided the rats into three groups:

The ZOL group (set no material in the tooth extraction fossa).

The Hep/GelMA group (set Hep/GelMA hydrogel in the tooth extraction fossa).

The Hep/GelMA-PRF group (set Hep/GelMA-PRF hydrogel in the tooth extraction fossa).

The other 12 SD rats were treated with an IP injection of the same amount of saline for six weeks (set no material in the tooth extraction fossa). All of them were postoperative intramuscular injections of penicillin (80000 U/kg) for three consecutive days (Fig. 7e, f).

### Micro-CT imgaging

The X-ray machine and Micro-CT were used to scan the imaging system to evaluate the bone. The X-ray machine adopts the parallel projection mode, 10 cm away from the focus, and the exposure time is 0.18 s. The Quantum GX2 micro-CT Imaging System was used to scan the system with a working voltage of 90 kV and a resolution of 17 μm. The region of interest was the first molar extraction fossa. The CTvox and DataViewer were used to observed the sample shape. The trabecular metric parameters measured included trabecular BMD, BV/TV, Tb.Th, and Tb.Sp.

### Histologic analysis

The mandible tissues were stained with hematoxylin and eosin staining kit (Solaibio, china), Masson's trichrome staining kit (Solaibio, china), Trap staining kit (Sigma, USA), and immunohistochemistry reagent (Maxim china). The sections were imaged under an OLYMPUS, BX53F microscope. The OLYMPUS cellSens Entry 2.2 software was used to analyze. In the expression analysis of immunohistochemically stained sections of different groups, the same area and the same conditions were selected for positive area analysis using Image J software.

### Statistics

Data were expressed as the mean ± standard error (SEM) using GraphPad Prism 9.5. All experiments were performed independently at least three times. The normal data distribution was assessed using the Shapiro–Wilk test. For data normally distributed, a t-test was used to compare two groups and one-way ANOVA was used to analyze significant differences among groups. When $p<0.05$, the results were significantly different.

## Conclusion

The constructed photo crosslinked Hep/GelMA hydrogel supported by PRF has excellent physical and chemical properties and good biocompatibility. It provides a stable microenvironment for tissue remodeling, prevents the invasion of foreign bacteria, and reduces the risk of infection. At the same time, it gives time and space to support the formation of new bone tissue in the tooth extraction fosse. Hep/GelMA-PRF hydrogel can effectively prevent the occurrence and progression of MRONJ in rats and is a promising tissue engineering material.

#### Acknowledgements

Parts of the figure were drawn by using pictures from Servier Medical Art. Servier Medical Art by Servier is licensed under a Creative Commons Attribution 3.0 Unported License. (https://creativecommons.org/licenses/by/3.0/)

#### Author contributions

Lu Tao: Conceptualization; data curation; methodology; project administration; supervision; software; writing – original draft; writing – review and editing. Ying Gao: Conceptualization; data curation; formal analysis; methodology; writing – original draft. Yushen Li: Formal analysis; methodology; resources; software. Liuqing Yang: Data curation; formal analysis; methodology; validation. Jingjing Yao: Methodology; resources; software; validation; visualization. Handan Hhuang and Jinling Yu: Investigation; methodology; supervision; validation; visualization. Bing Han: Data curation; formal analysis; methodology; resources; writing – review and editing. Bowei Wang and Zhihui Liu: Conceptualization; funding acquisition; investigation; methodology; project administration; resources; supervision; writing – review and editing.

#### Funding

This research was funded by the General Program of National Natural Science Foundation of China (Grant No. 82370934). This research was funded by the Science and Technology Department of Jilin Province (Grant No. 20220401102YY). This research was funded by the Science and Technology Department of Jilin Province (Grant No. 20230204076YY). This research was funded by the Graduate Innovation Fund of Jilin University (Grant No.2022241).

#### Data availability

The datasets used and/or analysed during the current study available from the corresponding author on reasonable request.

## Declarations

#### Ethics approval and consent to participate

The experiments were done under the guidelines and regulations of ARRIVE guidelines. Carried out all animal-related experiments in the Laboratory Animal Center of Jilin University. Reviewed and approved all experiments by the Institutional Animal Care and Use Committee and complied with Jilin University's and the state's requirements for the ethical welfare of experimental animals (China, Protocol number: SYXK2023-0010). Controlled the breeding conditions in strict accordance with GB14925.

#### Consent for publication

Not applicable.

#### Competing interests

The authors declare no competing interests.

#### Author details

[1]Hospital of Stomatology, Jilin University, Changchun 130021, People's Republic of China
[2]Jilin Provincial Key Laboratory of Tooth Development and Bone Remodeling, Changchun 130021, People's Republic of China
[3]The Second Hospital of Jilin University, Changchun 130041, People's Republic of China
[4]Department of Biopharmacy, School of Pharmaceutical Sciences, Jilin University, Changchun 130021, People's Republic of China

Received: 1 March 2024 / Accepted: 22 August 2024
Published online: 29 August 2024

**References**

1. Barbosa JS, Almeida Paz FA, Braga SS, Bisphosphonates. Old friends of bones and New trends in clinics [J]. J Med Chem. 2021;64(3):1260–82.
2. Reid IR. Billington EO. Drug therapy for osteoporosis in older adults [J]. Lancet (London England). 2022;399(10329):1080–92.
3. Kuznik A, Pazdzierniok-Holewa A, Jewula P et al. Bisphosphonates-much more than only drugs for bone diseases [J]. Eur J Pharmacol, 2020, 866.
4. Diab DL, Watts NB. Bisphosphonate drug holiday: who, when and how long [J]. Therapeutic Adv Musculoskelet Disease. 2013;5(3):107–11.
5. Papapoulos SE, Cremers SCL, M. Prolonged bisphosphonate release after treatment in children [J]. N Engl J Med. 2007;356(10):1075–6.
6. Baron R, Ferrari S, Russell RGG. Denosumab and bisphosphonates: different mechanisms of action and effects [J]. Bone. 2011;48(4):677–92.
7. Ruggiero SL, Dodson TB, Fantasia J, et al. American Association of Oral and maxillofacial surgeons position paper on medication-related osteonecrosis of the Jaw-2014 update [J]. J Oral Maxillofac Surg. 2014;72(10):1938–56.
8. Ruggiero SL, Dodson TB, Aghaloo T, et al. American Association of Oral and Maxillofacial Surgeons' Position Paper on Medication-Related Osteonecrosis of the Jaw-2022 Update [J]. Journal of oral and maxillofacial surgery. official journal of the American Association of Oral and Maxillofacial Surgeons; 2022.
9. Marx RE. Pamidronate (Aredia) and zoledronate (Zometa) induced avascular necrosis of the jaws: a growing epidemic [J]. J Oral Maxillofac Surg. 2003;61(9):1115–7.
10. Taysi AE, Cevher E, Sessevmez M et al. The efficacy of sustained-release chitosan microspheres containing recombinant human parathyroid hormone on MRONJ [J]. Brazilian Oral Res, 2019, 33.
11. Hadad H, Kawamata de Jesus L, Piquera Santos AF et al. Beta tricalcium phosphate, either alone or in combination with antimicrobial photodynamic therapy or doxycycline, prevents medication-related osteonecrosis of the jaw [J]. Sci Rep, 2022, 12(1).
12. Gonen ZB, Asan CY. Treatment of bisphosphonate-related osteonecrosis of the jaw using platelet-rich fibrin [J]. Cranio-the J Craniomandib Sleep Pract. 2017;35(5):332–6.
13. Maluf G, Caldas RJ, Silva Santos PS. Use of leukocyte- and platelet-rich fibrin in the treatment of medication-related osteonecrosis of the Jaws [J]. J Oral Maxillofac Surg. 2018;76(1):88–96.
14. Szentpeteri S, Schmidt L, Restar L, et al. The effect of platelet-rich fibrin membrane in Surgical Therapy of Medication-related osteonecrosis of the Jaw [J]. J oral Maxillofacial Surgery: Official J Am Association Oral Maxillofacial Surg. 2020;78(5):738–48.
15. Choukroun J, Diss A, Simonpieri A, et al. Platelet-rich fibrin (PRF): a second-generation platelet concentrate. Part V: histologic evaluations of PRF effects on bone allograft maturation in sinus lift [J]. Oral Surg Oral Med Oral Pathol Oral Radiol Endodontology. 2006;101(3):299–303.
16. Jamalpour MR, Shahabi S, Baghestani M et al. Complementarity of surgical therapy, photobiomodulation, A-PRF and L-PRF for management of medication-related osteonecrosis of the jaw (MRONJ): an animal study [J]. BMC Oral Health, 2022, 22(1).
17. Benoit DSW, Anseth KS. Heparin functionalized PEG gels that modulate protein adsorption for hMSC adhesion and differentiation [J]. Acta Biomater. 2005;1(4):461–70.
18. van den Bulcke AI, Bogdanov B, de Rooze N, et al. Structural and rheological properties of methacrylamide modified gelatin hydrogels [J]. Biomacromolecules. 2000;1(1):31–8.
19. Liu, Y, Chan-Park MB. A biomimetic hydrogel based on methacrylated dextran-graft-lysine and gelatin for 3D smooth muscle cell culture [J]. Biomaterials. 2010;31(6):1158–70.
20. Zhang J, Liu X, Ma K, et al. Collagen/heparin scaffold combined with vascular endothelial growth factor promotes the repair of neurological function in rats with traumatic brain injury [J]. Biomaterials Sci. 2021;9(3):745–64.
21. Lewiecki EM. Safety of long-term bisphosphonate therapy for the management of osteoporosis [J]. Drugs. 2011;71(6):791–814.
22. Wysowski DK Greenep. Trends in osteoporosis treatment with oral and intravenous bisphosphonates in the United States, 2002–2012 [J]. Bone. 2013;57(2):423–8.
23. Anwandter A, Bohmann S, Nally M, et al. Dimensional changes of the post extraction alveolar ridge, preserved with leukocyte- and platelet Rich Fibrin: a clinical pilot study [J]. J Dent. 2016;52:23–9.
24. Scott JE, Dorling J. Differential staining of acid glycosaminoglycans (mucopolysaccharides) by alcian blue in salt solutions [J]. Histochemie Histochem Histochimie. 1965;5(3):221–33.
25. Yan R, Jiang R. Hu L, Establishment and assessment of rodent models of medication-related osteonecrosis of the jaw (MRONJ) [J]. Int J Oral Sci, 2022, 14(1).
26. Reid IR, Green JR, Lyles KW et al. Zoledronate [J] Bone, 2020, 137.
27. Huang J, Wang L. Small extracellular vesicles derived from adipose tissue prevent bisphosphonate-related osteonecrosis of the Jaw by promoting angiogenesis [J]. Int J Nanomed. 2021;16:3161–72.
28. Messer JG, Calle JLM, Jiron JM, et al. Zoledronic acid increases the prevalence of medication-related osteonecrosis of the jaw in a dose dependent manner in rice rats (Oryzomys palustris) with localized periodontitis [J]. Bone. 2018;108:79–88.
29. Yu W, Su J. The effects of different doses of teriparatide on bisphosphonate-related osteonecrosis of the jaw in mice [J]. Oral Dis. 2020;26(3):609–20.
30. Williams DW, Lee C, Kim T, et al. Impaired bone resorption and woven bone formation are Associated with Development of Osteonecrosis of the Jaw-Like lesions by Bisphosphonate and Anti-receptor Activator of NF-kappa B ligand antibody in mice [J]. Am J Pathol. 2014;184(11):3084–93.
31. Du W, Yang M, Kim T et al. Indigenous microbiota protects development of medication-related osteonecrosis induced by periapical disease in mice [J]. Int J Oral Sci, 2022, 14(1).
32. Kim T, Kim S, Song M, et al. Removal of pre-existing Periodontal Inflammatory Condition before tooth extraction ameliorates medication-related osteonecrosis of the Jaw-Like Lesion in mice [J]. Am J Pathol. 2018;188(10):2318–27.
33. Liu Y, Cox SR, Morita T, et al. Hypoxia regulates vascular endothelial growth factor gene expression in endothelial cells. Identification of a 5′ enhancer [J]. Circul Res. 1995;77(3):638–43.
34. Ozalp O, Yildirimyan N, Ozturk C et al. Promising results of surgical management of advanced medication related osteonecrosis of the jaws using adjunctive leukocyte and platelet rich fibrin [J]. BMC Oral Health, 2021, 21(1).
35. Tenore G, Zimbalatti A, Rocchetti F et al. Management of medication-related osteonecrosis of the Jaw (MRONJ) using leukocyte- and platelet-rich fibrin (L-PRF) and photobiomodulation: a retrospective study [J]. J Clin Med, 2020, 9(11).
36. Yarom N, Shapiro CL, Peterson DE, et al. Medication-related osteonecrosis of the Jaw: MASCC/ISOO/ASCO Clinical Practice Guideline [J]. J Clin Oncol. 2019;37(25):2270–.
37. Bennardo F, Gallelli L, Palleria C et al. Can platelet-rich fibrin act as a natural carrier for antibiotics delivery? A proof-of-concept study for oral surgical procedures [J]. BMC Oral Health. 2023;23(1).

## Publisher's note